Atmos. Chem. Phys. Discuss., https://doi.org/10.5194/acp-2017-634
Manuscript under review for journal Atmos. Chem. Phys.
Discussion started: 24 August 2017

New insights into the vertical structure of the September 2015 dust storm employing 8 ceilometers over Israel

Leenes Uzan[1,2], Smadar Egert[1], Pinhas Alpert[1]

[1] Department of Geosciences, Raymond and Beverly Sackler Faculty of Exact Sciences, Tel-Aviv University, Tel Aviv, 6997801, Israel.
[2] The Israeli Meteorological Service, Beit Dagan, Israel.

Correspondence to: Leenes Uzan (Leenesu@gmail.com)

Atmos. Chem. Phys. Discuss., https://doi.org/10.5194/acp-2017-634
Manuscript under review for journal Atmos. Chem. Phys.
Discussion started: 24 August 2017

Atmospheric Chemistry and Physics
Open Access
Discussions

Abstract

On September 7th 2015, an unprecedented dust storm approached the East Mediterranean (EM) basin. The storm origin was in the Iran, Iraq, Syria and the Turkey border. The Israeli meteorological service considered the storm as exceptional due to its extent of over 6 days, occurrence time in early September and concentrations reaching values 100 times the normal. Previous studies examined the formation and evolution of the dust storm synoptic scale and explained why aerosol models often failed to simulate it. This study concentrates on spatial and vertical meso-scale dust spreading over Israel based on several remote sensing instruments including eight micro light detection and ranging (LIDAR) ceilometers. The ceilometers high resolution attenuated backscatter profiles (every 10 m and 15 s) reveal the downward motion of elevated dust plume as it penetrated Israel, ground coverage and gradual dispersion. The additional data of spectral radiometers and ground particulate matter under 10 micro-meter aero-diameter (PM10) as well as meteorological data made it possible to verify the dust properties and the differences between its ground deposition and elevated dispersion. Further investigations of dust storms in the EM by the ceilometer array will help improve the regional forecast models.

1. Introduction

Dust storms in the East Mediterranean (EM), defined as Sharav cyclones, are common through the months of April, May, October and December (Alpert and Ziv, 1989). As the Sharav cyclone travels rapidly eastwards from North Africa to the EM, dry hot air enters Israel generating dust plumes which typically last 1-2 days, doubling the monthly average surface dust concentration (Israeli Environmental ministry air quality, monthly reports).

The September 2015 dust storm was created north east to Israel, in the beginning of September (Fig. 1). Dust advections from the northeast do not occur in the summer season nor do they result with such a major dust impact (Israeli Meteorological Service monthly reports). In the September dust storm, high ground-level particulate matter concentrations were measured for over 3 days with the highest levels of 100 times above the hourly average of 60 μg/m^3 in Jerusalem (Israeli Environmental ministry air quality monthly reports). Low visibility of 0.5-3 km was measured across the county for four consecutive days during 8-11 Sep 2015 (Israel Meteorological Service monthly reports, AErosol RObotic NETwork (AERONET) radiometers).

Atmos. Chem. Phys. Discuss., https://doi.org/10.5194/acp-2017-634
Manuscript under review for journal Atmos. Chem. Phys.
Discussion started: 24 August 2017

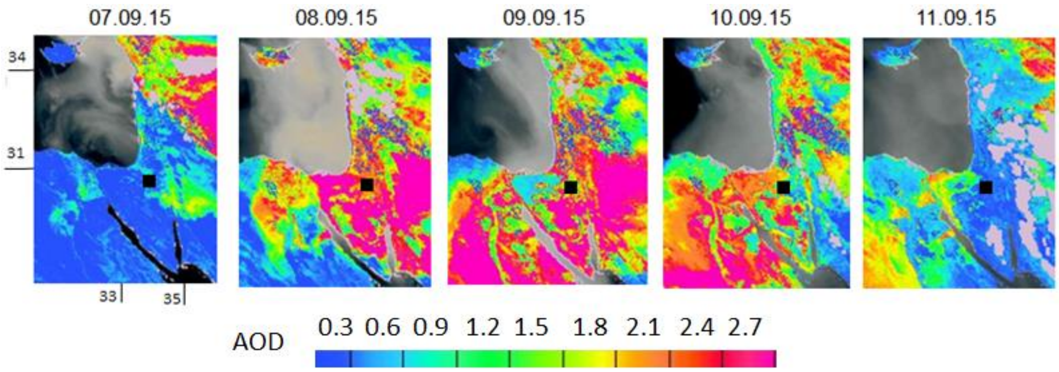

Figure 1. Aerosol Optical Depth (AOD) at 12 UTC from Meteosat Second Generation (MSG) spacecraft. The black square indicates the location of the Sede-Boker AERONET unit measuring AOD from ground level. The AOD measurements are given in Fig. 6.

Jasmin (2016) compared the dust storm aerosol content provided by Meteosat Second Generation (MSG) by the Spinning Enhanced Visible and InfraRed Imager (SEVIRI) observations, to the results of the open source Meteoinfo model. The Meteoinfo model was based on meteorological variables from the European Centre for Medium-Range Weather Forecasts (ECMWF). The meteorological conditions generated by the model suggested a formation of two dust storms simultaneously, from northern Syria and the Egyptian Sinai desert as a result of updrafts created by low pressure systems.

Mamouri et al (2016), analyzed the dust storm development in the Cyprus region based on Moderate Resolution Imaging Spectroradiometer (MODIS) aboard the Aqua satellite (MODIS-Aqua). Aerosol Optical Depth (AOD) satellite pictures, backscatter and attenuation profiles based on a multispectral LIDAR from the European Aerosol Research LIDAR Network (EARLINET), and ground level measurements of PM10. They concluded that the dust plumes from Syria entered the EM in a double layer structure, 1.5 and 4 km above sea level (ASL), pointing out to the possibility of multiple dust sources.

Gasch et al. (2016) claimed an unusual early incidence of an active Red Sea Trough (RST, Fig. 2c) (Alpert et al, 2004) followed by meso-scale convective systems generating cold-pool outflows producing the dust storms (Fig. 2c). They applied the ICOsahedral Nonhydrostatic (ICON) modelling system with the Aerosol and Reactive Trace gases (ART). This model better explained the dust evolution but lacked sufficient development of a super critical flow in order to produce the excessive surface wind speeds. These eventually misled the forecast of the dust advection southwest into Israel.

The model results were related to two Cloud-Aerosol LIDAR and Infrared Pathfinder Satellite Observation (CALIPSO) LIDAR overpasses (Winker et al., 2009). They suggested that the dust plume expanded north-west and then turned south-east as the trough collapsed penetrating Israel and Egypt from the east. In addition, they related the model findings with three particulate matter ground station measurements in Israel.

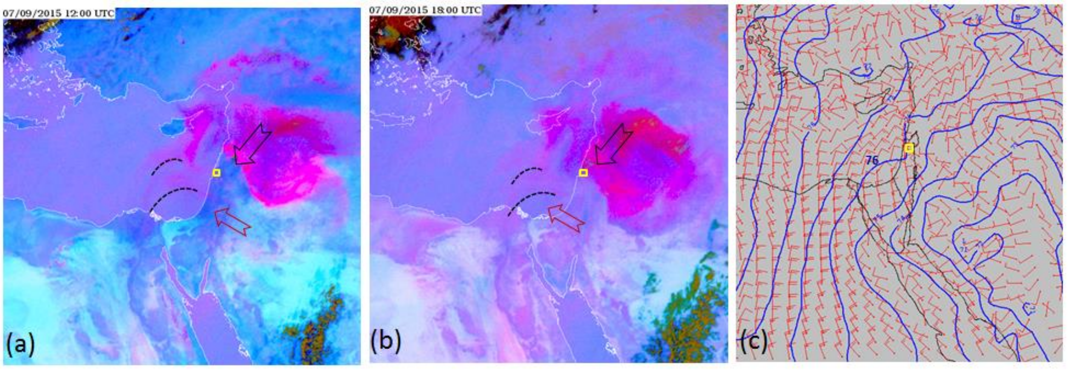

Figure 2. MSG-SEVIRI satellite pictures of dust RGB component at 07.09.15 12 UTC (a) and 18 UTC (b). The dust appears in pink colors. Indications of the Mount Meron site (Yellow Square at Lon 33.0˚ Lat 35.4˚) the first dust plume (red arrow and dashed line) and second dust plume (black arrow).
(c) Synoptic 925 mb 12 UTC map of the geopotential height with 1 dm interval (the 76 dm line is passing over Israel; blue lines) and wind (10 kt each line; red arrows).

Parolari et al. (2016), conducted simulations using the Weather Research and Forecasting (WRF) model that disclosed an unusual low level westerly wind spread to the EM, enhancing surface wind shear stress to reversely transport the previously eastward particles back to the EM.

Solomos et al. (2016) investigated the dust event by an EARLINET LIDAR, satellite aerosol content observations from MSG, and the CALIPSO. In addition, they ran the high regional atmospheric modeling system (RAMS) in order to reanalyze the progression of the dust event. The model results were compared with the satellite pictures and LIDAR measurements. The model predicted a few events of dust outbreaks resulting from different synoptic conditions. They have succeeded to improve the plumes extent and front directions compared to the original forecasts, but the ability to predict the details were partial, probably due to inaccuracies in the model physical processes. Eventually, the aerosol concentration profile of the improved model was lower than the actual LIDAR measurements.

Ginoux and Pu, (2016) studied the dust optical depth (DOD) derived by the deep blue algorithm aerosol product from MODIS aboard the Terra satellite (MODIS-Terra) and MODIS-Aqua The AOD 10 km resolution pictures from MODIS-Terra and MODIS-Aqua pictures, were combined with monthly horizontal winds and geopotential heights generated by the ECMWF reanalysis (horizontal resolution of 80 km and 37 vertical levels). The DODs were compared with the Geophysical Fluid Dynamics Laboratory (GFDL) Atmospheric model (AM3) with a horizontal resolution of 200 km, and vertical resolution from 70 m up to 4 km AGL (Donner et al., 2011) to produce AODs and scattering properties. Comparison between the model results and AOD AERONET measurements revealed the model underestimation particularly in the EM. Likewise, the model underestimated the DODs compared to satellite DODs. The authors assumed that these dissimilarities were due to inconsideration of the soil moisture parameter in the model.

A summary of the aforementioned studies is given in Table 1.

To this point, the forecast and reanalysis models were found to be incapable of reproducing the details of this extreme dust storm event. So far, no attempt has been done to relate the models findings to a continuous spatial, temporal and vertical set of profiles measurements. The goal here is to display the evolution of this extreme event by several local remote sensing devices available in Israel, particularly the eight ceilometers spread across Israel in order to describe the plume evolution.

An overview of the instruments and location of the measuring sites is given in Sect. 2. Section 3 presents the results. Conclusions and discussion are given in Sect. 4.

2. Instruments

Continuous measurements of aerosols in Israel are conducted by PM10 ground monitoring stations managed by the Israeli Environmental Protection ministry (IEPM). While the monitoring stations provide the temporal and spatial dispersion of the aerosols on ground level, AERONET measurements portrays several parameters of the aerosol content in the column of air from ground level to the atmosphere above its measuring point. Despite the progress with the satellite products from MODIS-Terra, MODIS-Aqua and MSG-SEVIRI, the 2D pictures cannot delineate the vertical evolution of the dust plume highly influenced by the spatial orography and particle distribution, governed by the synoptic system and meso-meteorological conditions (Su and Toon, 2011).

Fortunately, the ability to add the vertical aerosol distribution by ground remote sensing ceilometers is available in Israel. These instruments use the LIDAR principle as a tool for mapping worldwide dust movements (Ansmann et al., 2011; Mona et al., 2014).

2.1 Ceilometers

The Vaisala CL31 ceilometer (Wiegner et al., 2014; Mona et al., 2014; Weitkamp, 2005; Muenkel et al., 2004) is a pulsed elastic micro LIDAR, employing an Indium Gallium Arsenide (InGaAs) laser diode transmitter of near infrared wavelength (910 nm ±10 nm at 25˚C). In order to provide sufficient signal to noise ratio (SNR), a repetition rate of 10 kHz of short pulses are emitted to the atmosphere, in a measuring interval of two seconds (Vaisala ceilometer CL31 user's guide at http://www.vaisala.com). The backscatter transmissions collected by an avalanche photodiode (APD) receiver, are averaged to produce an individual attenuated backscatter profile, within a reporting interval of 2 to 120 s. The attenuated backscattering relative signals (profiles) were used in this study to verify the trends in the vertical distribution of the dust and its spreading over Israel. The diurnal mixed layer height (MLH) was evaluated by the wavelet covariance transform (WCT) method (Uzan, et al, 2016). Using this data together with the satellites pictures AOD and the spectral integrated AErosol RObotic NETwork (AERONET) measurements described below, made sure that only dust was addressed.

Based on the CL31 specifications it should measure linearly from ground level up to 7.7 km AGL. However, when the signals are analyzed it is clear that the instruments have a structured feature of an artificial peak around 50-100 m AGL (the exact location is instruments dependent). Since this feature is repeatable, it is possible to verify relative changes in the signal strength below this height, but linear measurements should be analyzed only above it. The CL31 features and their dependence on the instruments electronics and software version were studied in details by the TOPROF group (Kotthaus et al., 2016).

The location of the ceilometers deployed in Israel is given in Fig. 3 and Table 2. The ceilometers transmit every 16 sec and with height resolution of 10 m between 0-4.5 km. The shoreline ceilometers, however, transmit every 15 sec. The Beit Dagan Ceilometer measures up to 7.7 km.

Atmos. Chem. Phys. Discuss., https://doi.org/10.5194/acp-2017-634
Manuscript under review for journal Atmos. Chem. Phys.
Discussion started: 24 August 2017

Atmospheric Chemistry and Physics
Open Access
Discussions

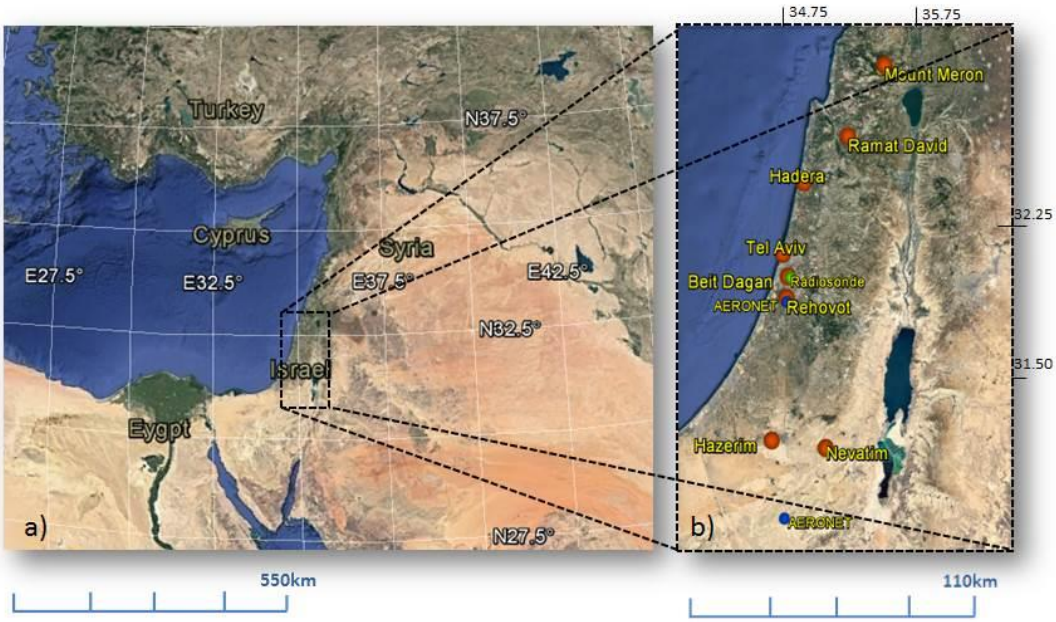

Figure 3. Google Earth map of 8 ceilometer deployment in Israel in 2015 (orange circle; detail in Table 2), two AERONET sites (blue circle; Sede-Boker & Rehovot-Weizmann) and the radiosonde launching site in Beit Dagan (green circle) at the site of Beit Dagan ceilometer.

2.2 Radiosonde

A radiosonde (RS) is a small instrument package suspended by a large hydrogen or helium gas balloon. As the radiosonde rises (~300 m/min) sensors on the radiosonde transmits pressure, temperature, relative humidity, wind speed, wind direction and GPS position data each second. In Israel the radiosonde is launched twice a day (00 UTC and 12 UTC) by the IMS, adjacent to the Beit Dagan ceilometer. The radiosonde files were downloaded from the University of Wyoming site (station number 40172). With respect to Stull (1988) the MLH was defined by the RS profiles as the height where the following phenomena where identified: an inversion layer in the temperature profile, a significant drop in the relative humidity profile, strong wind shear in the wind speed profile and an increase in the virtual temperature profile (Uzan et al., 2016; Levi et al., 2011).

Although the large scale and intensity of the event, the dust storm dynamics was quite different between neighboring countries. For example, the Israeli radiosonde profiles were compared to the nearest available radiosonde site in Cyprus (station number 17607). Details on launching sites are given in Table 3. Fig. 4 presents the temperature and relative humidity profiles from 07.09.15 to 10.09.15 between the

Atmos. Chem. Phys. Discuss., https://doi.org/10.5194/acp-2017-634
Manuscript under review for journal Atmos. Chem. Phys.
Discussion started: 24 August 2017

heights of 100-1,500 m AGL disclosing the different meteorological conditions in Israel and Cyprus in spite of a relatively short distance of about 350 km.

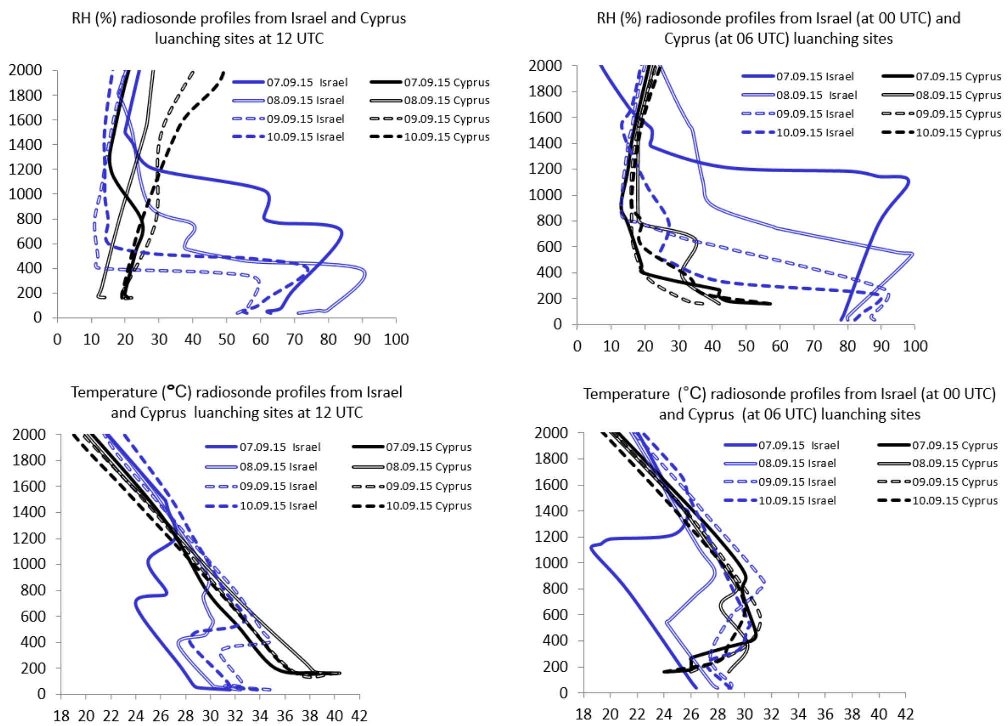

Figure 4. Radiosonde Temperature and Relative humidity (RH) profiles at 12 and 00 UTC from the Israeli launching site (blue profiles) and at 12 and 06 UTC from the Cyprus launching site (black profiles) between 07.09.15-10.09.15.

2.3 PM10

The majority of the ground particulate matter measurements in Israel are done by method of the beta attenuation. The beta attenuation monitor samples at ambient temperatures in a low-volume flow rate. Low-energy beta rays are focused on deposits on a filter tape and attenuated according to the approximate exponential function of particulate mass (i.e., Beer's Law). These automated samples employ a continuous filter tape. Typically, the attenuation through an unexposed portion of the filter tape is measured, and the tape is then exposed to the ambient sample flow where a deposit is accumulated. The beta attenuation is repeated, and the difference in attenuation between the blank filter and the deposit is a measure of the accumulated concentration. The PM10 monitors report 5 min average mass concentrations (IEPM monthly report).

An ensemble of 3-hourly average of PM10 concentration from 38 monitoring stations was analyzed. For convenience, we divided the monitoring stations into 4 geographical regions: east, center, shoreline and south (Fig. 5). Unfortunately, there are no PM10 measurements in northern Israel. The eastern region includes the highest monitoring stations up to 960 m ASL. Further detail of the PM10 measurement sites is given in Table 4. The average availability of PM10 data throughout the period of the dust storm, from 07.09.15 to 10.09.15, was relatively high, i.e., over 90% from 33 stations (87% of the monitoring stations Surprisingly, in all the geographical regions (except the east Mountain region, PM10 measurements indicated the dust event began on the 8.9.15. This will be discussed in detail in Sect. 3.

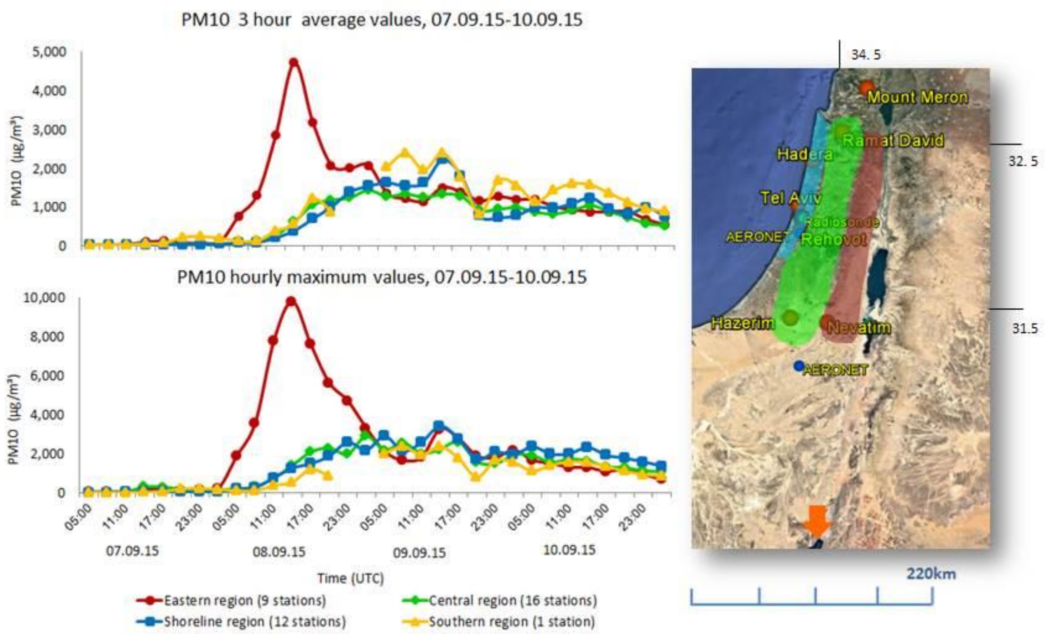

Figure 5. Map of PM10 geographical regions-right panel map: east (red), center (green), shoreline (blue) and south (orange arrow). The regions were overlaid upon the 8 ceilometer deployment map. The left panels are the PM10 measurements for the four regions with the same colors. The 3-h average concentration (upper panel) and 1-h maximum (lower panel). Notice the different PM10 concentration scale (double for the maximum). Time period is 07.09.15-10.09.15, time in UTC.

Atmos. Chem. Phys. Discuss., https://doi.org/10.5194/acp-2017-634
Manuscript under review for journal Atmos. Chem. Phys.
Discussion started: 24 August 2017

2.4 AERONET

AErosol RObotic NETwork (AERONET) is an automatic sun tracking radiometer which makes direct sun measurements every 15 min at 340, 380, 440, 500, 675, 870, 940, and 1020 nm wavelengths. The cycle of 8 wavelengths is scanned in 8 sec. Sequences of three measurements taken 30 s apart produce three measurements at each wavelength within a 1 min period. These solar extinction measurements are then used to compute aerosol optical depth at each wavelength except for the 940 nm channel, which is used to retrieve precipitable water in centimeters (Holben et al., 1998).

In Israel two AERONET units are operated in Sede-Boker and Weizmann Institute in Rehovot (Fig. 3), but only the Sede-Boker unit measured throughout the whole event (Fig. 6 in blue). The AERONET unit in Rehovot did not operate on the first two days of the dust storm (Fig. 6 in orange). The combination of high AOD and low Angström number indicate the dust event was comprised mainly by coarse particles of mineral dust (Dubovik et al., 2000; Kaskaoutis et al., 2008).

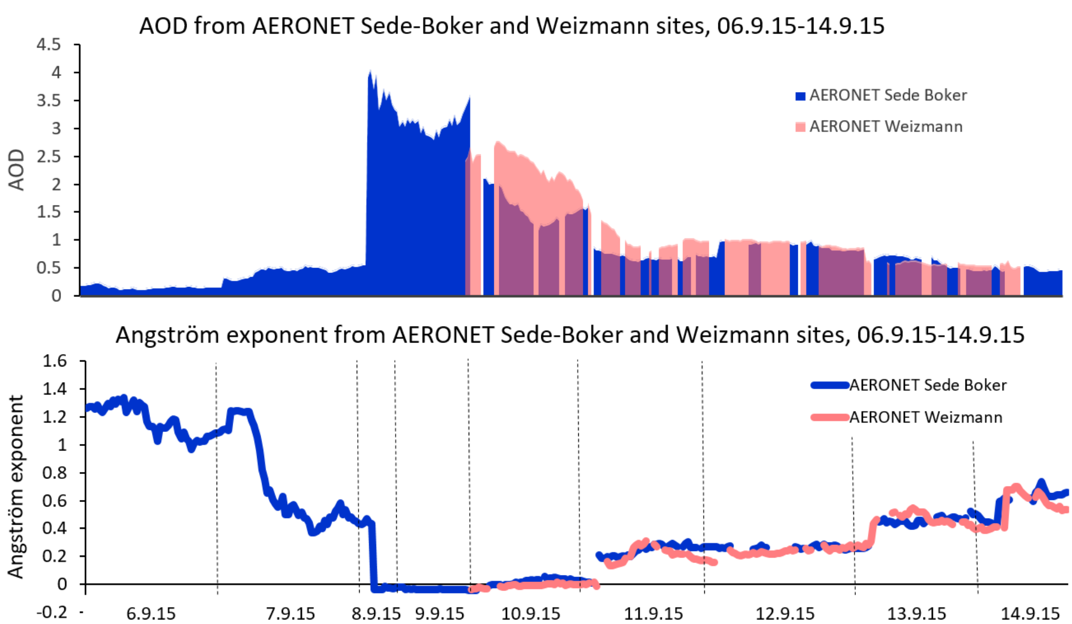

Figure 6. A combination of AERONET observations for 6.9.15-14.9.15 of AOD (top panel) and Angström exponent (bottom panel) from two measuring sites: Sede-Boker (southern Israel) and Weizmann Institute in Rehovot (central Israel). Both units did not operate consecutively. The Sede-Boker site operated throughout the dust event while the AERONET Weizmann site began operating from 9.9.15.

Atmos. Chem. Phys. Discuss., https://doi.org/10.5194/acp-2017-634
Manuscript under review for journal Atmos. Chem. Phys.
Discussion started: 24 August 2017

3. Results

The data collected by the ceilometers, AERONET radiometers, AOD satellite pictures and PM10 ground detectors was combined to describe the dust storm penetration and development over Israel. As a single wavelength instrument, ceilometers cannot distinguish between aerosols types. Therefore, the measured profiles were analyzed to distinguish between clouds and other aerosols. The ceilometer profiles are unitless and therefore divided by a scale factor of 10^{-9} m^{-1} sr^{-1} enabling quantitative analysis (Kotthaus et al., 2016). An example of the ability to distinguish attenuated backscatter profiles from clouds and dust plume is given in Fig. 7 with reference to Fig. 8. as follows: High signals of attenuated backscatter, up to $7*10^{-1}$ m^{-1} sr^{-1} were received on 7.9.15 (Fig. 7a, indicated arrow no.1 in Fig. 8). Profiles containing dust plume produced signals up to $4*10^{-5}$ m^{-1} sr^{-1} were received on the 07.09.15 (Fig. 7b, indicated by arrow no.2 in Fig. 8). The process on the 08.09.15 (Fig. 7c, indicated by arrow no.3 in Fig. 8) displays a double layer dust plume, at 250 m ASL of ~ 1*10 m^{-1} sr^{-1} and 450 m ASL of ~ $4*10^{-5}$ m^{-1} sr^{-1}. On 9.9.15 (Fig. 7d, indicated by arrow no.4 in Fig. 8) only a thin lofted plume is evident between 300-350 m ASL of ~$1.5*10^{-5}$ m^{-1} sr^{-1}.

Atmos. Chem. Phys. Discuss., https://doi.org/10.5194/acp-2017-634
Manuscript under review for journal Atmos. Chem. Phys.
Discussion started: 24 August 2017

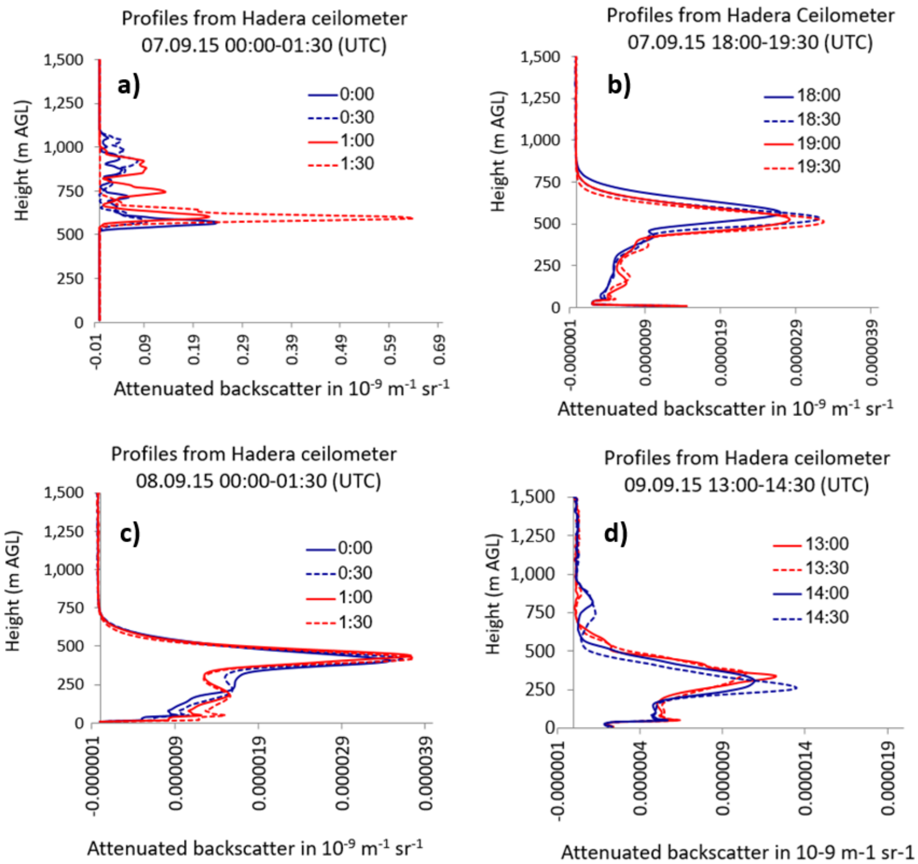

Figure 7. Hadera ceilometer attenuated backscatter profiles for cloud and dust plume detections indicated in Fig.8 by (a) arrow no.1 (clouds), (b) arrow no.2 (dust layer), (c) arrow no.3 (dust layer), d) arrow no.4 (dust layer).

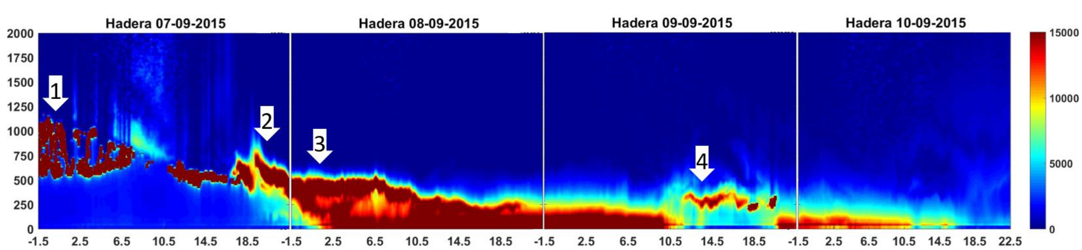

Figure 8. Hadera ceilometer attenuated backscatter plots for 07.09.15-10.09.15. y-axis is the height up to 2000 m AGL, x-axis is the time corrected from local time to UTC.

During the entire period of the dust event, both AERONET radiometers indicated growth of the coarse particle fraction in the size distribution and high absorption in the UV (400nm) region (not shown). These characteristics together with the satellite pictures indicated that the ceilometers tracked the dust entrance and evolution.

Mamouri et al. (2016) performed a coarse estimation of the extinction based on visibility measurements below ~500m at three different locations in Cyprus. Here, the estimation was done by the Koschmieder equation (Koschmieder 1924) based on the typical ~40-50 sr LIDAR ratio for dust, visibility measurements on the 8.9.15 of ~ 200 m (IMS reports). The estimated attenuated backscatter value matched the order of magnitude measured using the Vaisala ceilometer CL31 scaling factor of 10^{-9} m^{-1} sr^{-1} (not shown).

Ceilometers are not provided with an AOD upper limit value for signal reliability of the ceilometer profiles. Therefore, the validity of the ceilometer measurements during high AOD levels (08.09.15-10.09.15) was crucial. To verify ceilometer could measure correctly up 500 m AGL, MLH calculations were related to the Beit Dagan radiosonde measurements which were comparable (Fig. 9).

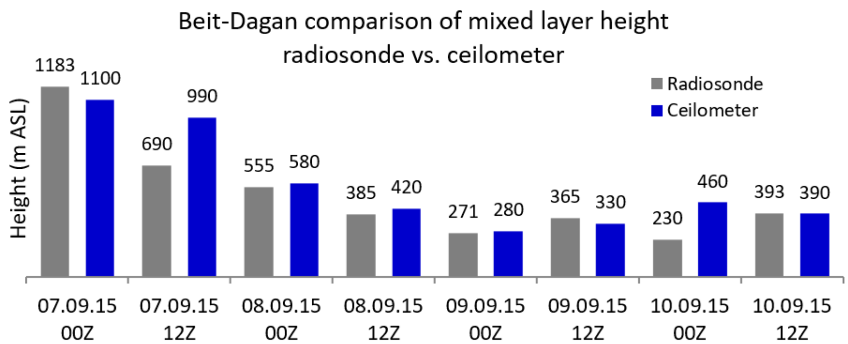

Figure 9. The mixed layer height over central Israel (Beit Dagan site) between 07.09.15-10.09.15 at 00 UTC and 12 UTC defined by adjacent radiosonde launches and ceilometer measurements, both in Beit Dagan site.

By the aforementioned tools, the dust event was analyzed as follows, providing consecutive ceilometer plots between 07.09.15-10.0915 (Fig. 8-16) from 8 sites (two for each region: north, shoreline, central and southern Israel). Notice the plots are given in different scale in order to highlight the dust feature in the different sites.

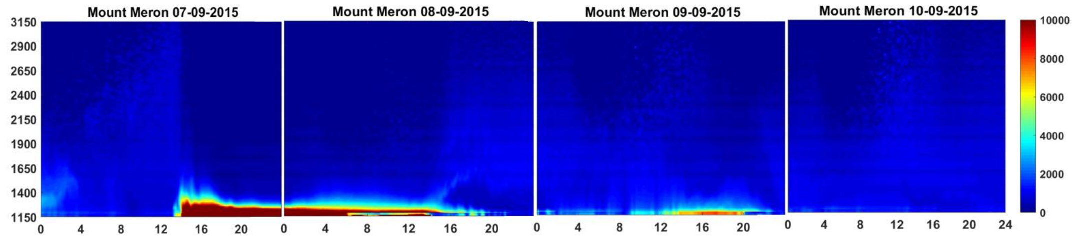

Figure 10. Same as Fig. 8 but for Mount Meron ceilometer site (Northern Israel,1150 m ASL). The x-axis is the time in UTC.

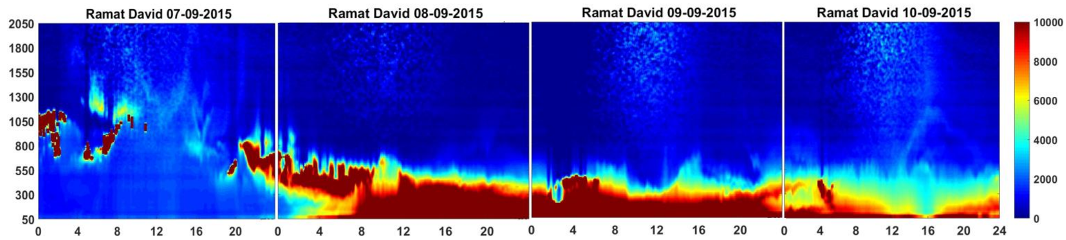

Figure 11. Same as Fig. 8 but for Ramat David ceilometer site (Northern Israel, 50 m ASL). The x-axis is the time in UTC.

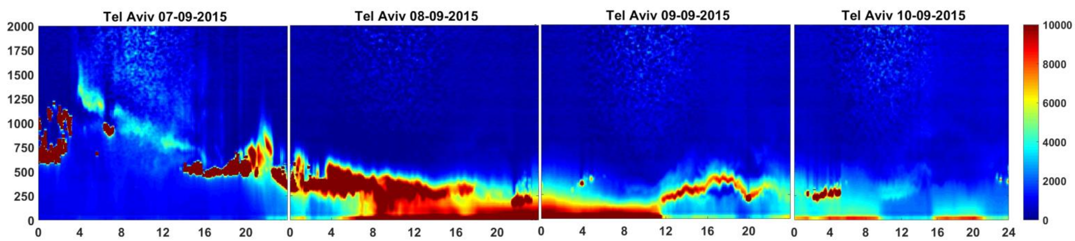

Figure 12. Same as Fig. 8 but for Tel Aviv ceilometer site (Israel shoreline, 5 m ASL). The x-axis is the time in UTC.

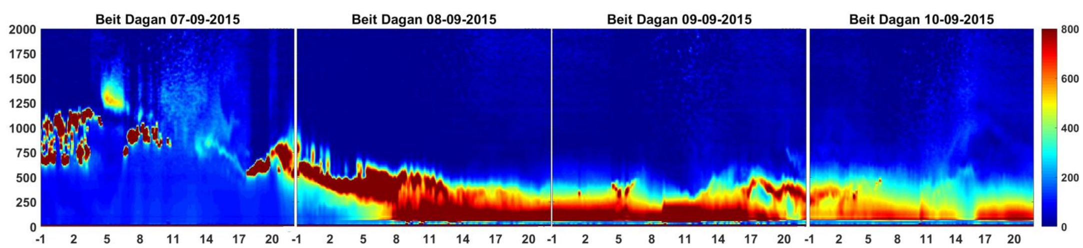

Figure 13. Same as Fig. 8 but for Beit-Dagan ceilometer site (Central Israel, 33 m ASL). The x-axis is the measurement time corrected from local time to UTC.

Atmos. Chem. Phys. Discuss., https://doi.org/10.5194/acp-2017-634
Manuscript under review for journal Atmos. Chem. Phys.
Discussion started: 24 August 2017

Atmospheric Chemistry and Physics
Open Access
Discussions
EGU

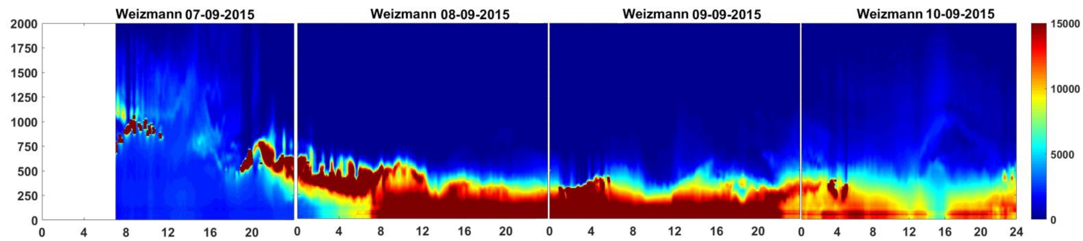

Figure 14. Same as Fig. 8 but for Weizmann ceilometer site in Rehovot (Central Israel, 60 m ASL). The x-axis is the time in UTC.

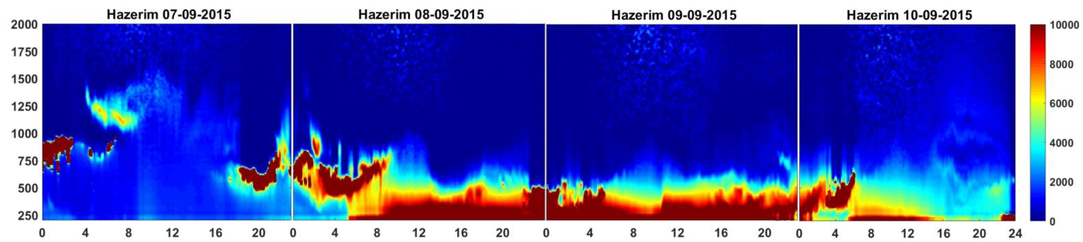

Figure 15. Same as Fig. 8 but for Hazerim ceilometer site (Southern Israel, 200 m ASL). The x-axis is the time in UTC.

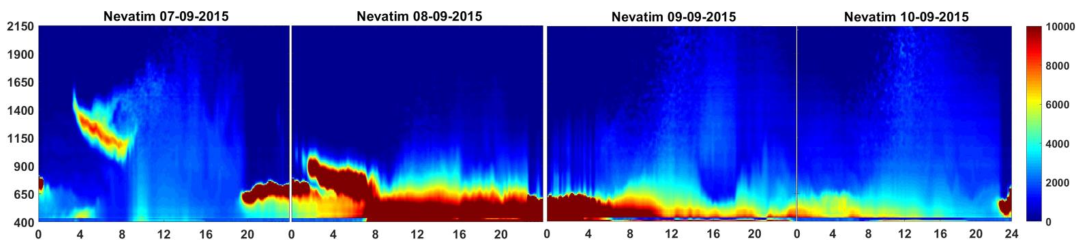

Figure 16. Same as Fig. 8 but for Nevatim ceilometer site (Southern Israel, 400 m ASL). The x-axis is the time in UTC.

Entrance of dust into Israel- 7 Sep 2015: Solomos et al. (2016) postulated that the dust storm was initially created as a dust front on the 06.09.15 as the result of a thermal low in Syria, north-east to Israel. This followed by a second front, generated by a thunder storm in northern Syria on the 07.09.15 giving rise to a fast running dust wall moving north-west then reaching Israel.

The AERONET (Fig. 6) and ceilometer plots (Fig. 8, 11-16) reveal that the first dust plume penetrated Israel at approximately 04:00 UTC at an elevated height of about 1500 m ASL. At this time, the ground station air monitoring 3-hourly PM10 concentration were still relatively low i.e., below 100 μg/m^3 (Fig. 5). The descending dust plume was measured by all ceilometers except for the Mount Meron ceilometer (Fig. 10). Indeed, the satellite pictures (Fig. 2 a, b) confirm that the first dust plume was fragmented and had not reached the region of Mount Meron before 12 UTC. Fig. 2c shows the corresponding 925 mb map including the deep RST intrusions to Syria and to Israel (Gasch et al., 2016).

The Mount Meron ceilometer, posted at 1150m ASL, captured the entrance of the second dust plume descending to approximately 1000m ASL at around 13:00 UTC. By then, the PM10 3-h concentration increased to 320 µg/m^3 (5 times the average) in the southeastern monitoring station in Beer-Sheva (270 m ASL; within the green zone, (Fig. 5) and 240 µg/m^3 in one of the highest monitoring stations in Jerusalem (800 m ASL; within the red zone, Fig. 4). Whereas in the shoreline, the PM10 concentrations were still low (blue zone; Fig. 5). Next, we describe the decrease of aerosols aloft on mid-day.

<u>Noon decrease of aerosols aloft- 7 Sep 2015</u>: The Israeli RS wind profiles on the 7.9.15 (not shown) rotated from north-east to the south-east at 1000-2000 m altitudes ASL. The change in wind direction disturbed the aforementioned dust plume descent, leading to dust dispersion over Israel. This is illustrated by the significant decrease of the dust in the ceilometer measurements (clearly shown in Fig. 13-16 between 08-16 UTC) while the particle deposition (PM10) was rising (Fig. 5). The ICON-ART model ran by Gasch et al., (2016) showed the dust plume split as it progressed to the south with one part descended through the Golan Heights. And, the other stretched south along the Red Sea Trough, rotating east as the wind altered along the trough margins. However, these model findings cannot explain the fact that both the elevated plume and the ground measurements began simultaneously at about 04 UTC.

<u>2nd day of dust event- 8 Sep 2015</u>: In the morning of 08.09.15, the AERONET in Sede-Boker discloses high AOD > 3. Ceilometers across the country (except to the Mount Meron site) disclose high and uneven vertically attenuated backscatter values of the dust in the atmosphere. This portioning occurred at approximately 07-08 UTC (Fig. 8, 11-16), as the surface mixed layer breaks and the thermals build up (Uzan and Alpert, 2012; Dayan et al., 2002). During the morning hours of the 08.09.15 the ground level PM10 concentration increased up to 9,800 µg/m^3 in Jerusalem which is 100 times over the 3 hourly normal average. The highest levels were measured mainly in the elevated monitoring stations, located on the high eastern strip of Israel (Fig. 5 and Table 4). These are represented only by the stations that were available in the south center part of Israel (due to the lack of PM10 measurements in the north). Radiosonde profiles show that the MLH subsides to 385 m ASL at 12 UTC (Fig. 9). The low MLH is accompanied by the increase of PM10 concentrations in all 38 PM10 stations, with the highest hourly value of ~2,000 µg/m^3 (Fig. 5).

The aforementioned earlier studies of this dust event employing both models and satellite pictures, had not clarified whether the descending plume was vertically mixed within the low MLH or rather merged with a dust wall that reached Israel. The process of the plume mixing can be verified from the vertical structures in Fig. 8-16 as follows. The ceilometers show that on the morning of the 08.09.15 (4-8 UTC) the dust profiles appeared as two separate dust layers-at near-ground and aloft (~500 m ASL) that have combined later in the morning (7-8 UTC).

<u>3rd day of dust event- 9 Sep 2015</u>: On the 09.09.15 a shallow MLH (Fig. 9) maintained the high PM10 concentrations e.g. 3,400 µg/m^3 in Hadera - 40 times over the average (Fig. 18) and high AOD > 3 (Fig 6). At approximately 11 UTC, the shoreline ceilometers (Tel Aviv and Hadera) revealed a discontinuous structure of a dust arc at (Fig. 8,12) which was less evident in the inland ceilometers in Beit-Dagan (Fig. 13) and Rehovot (Fig. 14). We presume the dust "arc" is a result of a dilution generated by the sea breeze front (SBF). The SBF entered at about 11 UTC (evaluated by the Tel Aviv onshore meteorological station, not shown) as limited radiative transmitted through the dense dust layer that had been covering Israel. Furthermore, prevailing northerly winds on the 09.09.15 restrained the SBF progress inland (not shown).

<u>4th day of dust event- 10 Sep 2015</u>: From 10.9.15 the ground level PM10 concentration decreased considerably (Fig. 5). Respectively, the ceilometers (Fig. 8-16) and satellite pictures (Fig. 1) show a decrease of the dust loads. Although ceilometer plots of the 10.09.15 reveal total clearance of the dust plume, the AERONET measurements from 14.09.15 show the AOD did not resume to the lowest values, prior to the dust storm. An example is given of the dust load dispersion between 11.09.15-14.09.15 in Fig. 17 from the Weizmann-Rehovot ceilometer.

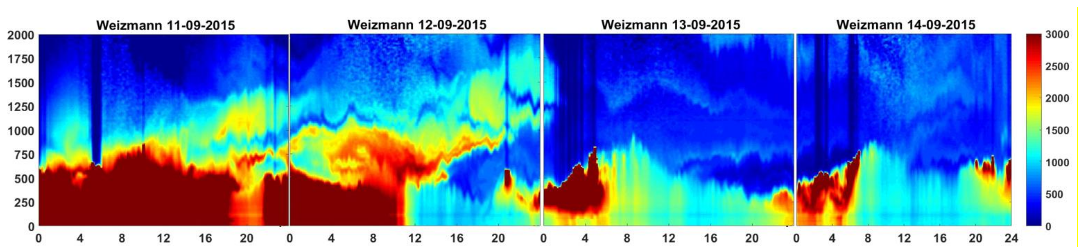

Figure 17. Weizmann ceilometer site in Rehovot (central Israel, 60 m AGL) attenuated backscatter plots between 11.09.15 - 14.09.15.Y-axis - heights up to 2000 m AGL, X-axis - time in UTC.

A Schematic evolution of the dust event is given in Fig. 18 as a dust layer of ~250 m (Fig 11-13, 15-16) penetrationed Israel at the height of ~ 1000-1500 m on 07.09.15 ~4 UTC. On the 08.09.17 the dust plume reached ground level height at about 08 UTC in the northern region (Fig 11, Ramat David ceilometer), central region (Fig- 13-14, Beit Dagan and Weizmann ceilometers) and shoreline strip (Fig 8 and 12, Hadera and Tel Aviv ceilometers). In the southern region (Hazerim and Nevatim ceilometers) the dust plume reached ground level earlier, beginning at 05 UTC. Correspondingly, an increase in PM10 concentration from the eastern region (Fig. 18) was measured by monitoring stations which are nearest to the southern ceilometers. The dissipation of the dust plume on 09.09.15-10.09.15 was revealed both by the dust features from the ceilometers plots (Fig. 8-16) and the decrease in PM10 concentration from adjacent monitoring station.

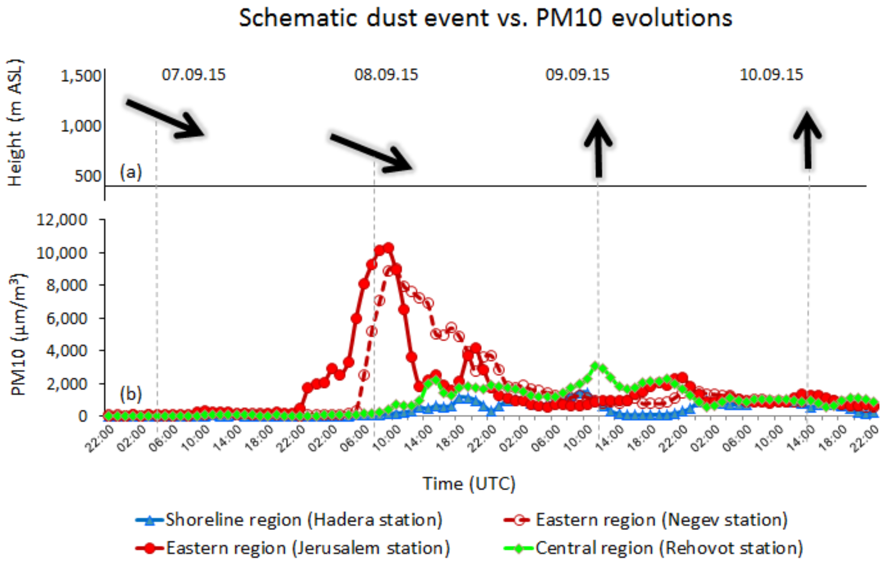

Figure 18**.** A schematic illustration of the dust storm evolution as discovered by the ceilometer plots (a, top panel), compared to the PM10 concentration (b, bottom panel) measured on ground level from four representative air monitoring stations (Hadera, Negev, Jerusalem and Rehovot) for the four regions (Shoreline, south, east and central, respectively, Fig. 5). The representative stations were chosen adjacent to corresponding ceilometer sites (Hadera, Nevatim, Beit-Dagan and Rehovot, respectively, Fig. 5)

4. Conclusions and discussion

Former research of the September 2015 dust event focused primarily on the synoptic evolution, outlined, the meteorological features and analyzed the limitations of the models to forecast such a dominant and unique event (Ginoux and Pu, 2016; Solomos et al, 2016; Parolari et al, 2016; Gasch et al, 2016; Jasmin, 2016; Mamouri et al, 2016). They had explained the dust storm progression by remote sensing means either looking from ground up (AERONET, PM10) or from space down (satellite).

In this study, for the first time, such an event is vertically analyzed using an array of ceilometers deployed across Israel. The ceilometer array enabled us to improve the the spatial the temporal evaluation and evolution of the September 2015 dust storm over Israel.

Beginning from the dust plum penetration to Israel from north-east (~ 1-1.5 km AGL) on the 07.09.15 reaching ground level height on the 08.09.15, creating a very low (beneath 500 m AGL) and stable MLH. As a result, extreme AOD values comprised mainly of mineral dust (Fig. 6), and high ground level PM10 concentrations were measured across Israel (Fig. 5). The highest values PM10 (100 times over the 3 hourly average) were measured on the 08.09.15 mainly in the elevated monitoring stations situated in the eastern strip of Israel. The clearance of the dust plum began in the shoreline on the 09.09.15 at approximately 11 UTC (Fig. 8) and continued on for several days until low AOD and high Angström values (indicating low content of mineral dust) finally resumed. During the clearing period, there were temporal and vertical differences in the dust plume evolution between the onshore and inland stations. These were attributed to the unusual late and weak sea breeze penetration due to the heavily opaque atmosphere. Detailed analysis of the various station vertical structure revealed the turbulent nature of the dust penetration attributed to the height and distance from seashore. These details were not revealed by the high resolution scale models.

The dust event measured in Cyprus (Mamouri et al., 2016) by an intensified LIDAR showed a structure of two dust layers, 1.5 and 4 km AGL. The complicated nature of the dust evolution and its creation, made it difficult to state if the same double layer structure reached Israel (and not measured by the CL31 ceilometers due to high SNR above 2 km) or was it partially carried by the different prevailing wind regimes over Israel and Cyprus (therefore, not measured even in the elevated Mount Meron site, 1150 m AGL).

Finally, this research emphasized the importance of LIDAR networks close to dust source areas such as the EM as a tool to improve forecast details and validate forecast models

5. Data availability

PM10 measurements- Israeli Environmental ministry air quality monthly reports: http://www.svivaaqm.net.
Weather reports- Israeli Meteorological Service monthly reports: http://www.ims.gov.il.
Radiosonde profiles –University of Wyoming: http://weather.uwyo.edu/upperair/sounding.html.
AERONET data- https://aeronet.gsfc.nasa.gov.
Meteosat Second Generation Spacecraft pictures: http://nascube.univ-lille1.fr/cgi-bin/NAS3_v2.cgi.
Ceilometer profiles- the data is owned by the Israeli defense force and the Israeli meteorological service. The data is not online and provided by request.

Author contribution

Leenes Uzan carried out the research and prepared the manuscript under the careful guidance of Smadar Egert and Pinhas Alpert. The authors declare that they have no conflict of interest.

Acknowledgements

We wish to thank the Israeli Meteorological Service (IMS), the Israeli Air Force (IDF), the Weizmann institute of science, the Association of towns for environmental protection (Sharon-Carmel) for their ceilometer data and collaboration. Special thanks to Anat Baharad, for the assistance with the MATLAB scripts, to Nir Stav and Dr. Yoav Levy (IMS) for their fruitful advice and data. We thank the principal investigators Prof. Arnon Karnieli and Prof. Yinon Rudich for their effort in establishing and maintaining Sede-Boker and Weizmann AERONET sites. We wish to thank the institutes that provide open site data reduction: NAScube, Wyoming University Radiosonde site and Israeli ministry of Environmental protection for the PM10 data. Expense of this research was partly funded by the Virtual Institute DESERVE (Dead Sea Research Venue).

References

Alpert P., Osetinsky I., Ziv B. and Shafir H.: A new seasons definition based on the classified daily synoptic systems: An example for the Eastern Mediterranean, Int. J. Climatol. 24,1013-1021, 2004.

Alpert, P., Ziv, B.: The Sharav cyclone-observations and some theoretical considerations, Int. J. Geoph. Res., 94, 18495-18514, 1998.

Continuous measurement of PM10 suspended particulate matter (SPM) in ambient air, Center for Environmental Research Information Office of Research and Development U.S. Environmental Protection Agency Cincinnati, OH 45268 June 1999.

Dayan U., Lifshitz-Golden B., and Pick K.: Spatial and structural variation of the atmospheric boundary layer during summer in Israel-profiler and rawinsonde measurements, J. Appl. Meteo. 41, 447-457, 2002.

Derimian, Y., Karnieli, A., Kaufman, Y.J., Andreae, M.O., Andreae, T.W., Dubovik, O., Maenhaut, W., Koren, I. and Holben, B.N.: Dust and pollution aerosols over the Negev desert, Israel: Properties, transport, and radiative effect, J. Geophys. Res., 111, D05205 (1-14), 2006.

Donner, L.J., Wyman, B.L., Hemler, R.S., Horowitz, L.W., Ming, Y., Zhao, M., Golaz, J.C., Ginoux, P., Lin, S.J., Schwarzkopf, M.D. and Austin, J.: The dynamical core, physical parameterizations, and basic simulation characteristics of the atmospheric component AM3 of the GFDL global coupled model CM3, Journal of Climate, 24(13), 3484-3519, 2011.

Dubovik, O., A. Smirnov, B. N. Holben, M. D. King, Y. J. Kaufman, T. F. Eck, and Slutsker I.: Accuracy assessments of aerosol optical properties retrieved from Aerosol Robotic Network (AERONET) Sun and sky radiance measurements, J. Geophys. Res., 105(D8), 9791–9806, 2000.

Gasch, P., Rieger, D., Walter, C., Khain, P., Levi, Y., and Vogel, B.: An analysis of the September 2015 severe dust event in the Eastern Mediterranean, Atmos. Chem. Phys. Discuss., in review, 2017.

Holben, B.N., Eck, T.F., Slutsker, I., Tanre, D., Buis, J.P., Setzer, A., Vermote, E., Reagan, J.A., Kaufman, Y.J., Nakajima, T. and Lavenu, F.: AERONET—A federated instrument network and data archive for aerosol characterization. Remote sensing of environment, 66(1), 1-16, 1998.

Jasim, F.H., Investigation of the 6-9 September 2015 Dust Storm over Middle East, AJER, 5 (11), 201-207, 2016.

Kaskaoutis, D.G., Kambezidis, H.D., Nastos, P.T. and Kosmopoulos, P.G.: Study on an intense dust storm over Greece. Atmospheric Environment, 42(29), 6884-6896, 2008.

Kotthaus, S., O'Connor, E., Münkel, C., Charlton-Perez, C., Gabey, A. M., and Grimmond, C. S. B.: Recommendations for processing atmospheric attenuated backscatter profiles from Vaisala CL31 Ceilometers. Atmos. Meas. Tech., 9, 3769-3791, 2016.

Koschmieder H.: Theorie der horizontalen sichtweite, Beitrage zur Physik der Freien Atmosphare 12, 33–55,171–181, 1924.

Levi Y., Shilo E., Setter I.: Climatology of a summer coastal boundary layer with 1290-MHz wind profiler radar and a WRF simulation. J. Appl. Meteo., 50(9), 1815-1826, 2011.

Mamouri, R.E., Ansmann, A., Nisantzi, A., Solomos, S., Kallos, G. and Hadjimitsis, D.G.: Extreme dust storm over the eastern Mediterranean in September 2015: satellite, LIDAR, and surface observations in the Cyprus region, Atmos. Chem. Phys., 16(21), 13711-13724, 2016.

Münkel C., Emeis S., Muller J. W., Schäfer K.: Aerosol concentration measurements with a LIDAR ceilometer: results of a one year measuring campaign, Remote sensing of Clouds and the Atmosphere VIII, 5235, 486-496, 2004.

Parolari, A.J., Li, D., Bou-Zeid, E., Katul, G.G. and Assouline, S.: Climate, not conflict, explains extreme Middle East dust storm, Environ. Res. Lett, 11, 114013, 2016.

Pu, B. and Ginoux, P.: The impact of the Pacific Decadal Oscillation on springtime dust activity in Syria, Atmos. Chem. Phys., 16(21), 13431-13448, 2016.

Solomos, S., Ansmann, A., Mamouri, R.-E., Binietoglou, I., Patlakas, P., Marinou, E., and Amiridis, V.: Remote sensing and modeling analysis of the extreme dust storm hitting Middle East and Eastern Mediterranean in September 2015, Atmos. Chem. Phys., 17, 4063-4079, 2017.

Stull R. B.: An introduction to boundary layer meteorology, Kluwer Academic publishers, Netherlands, 666p, 1988.

Uzan L., Alpert P.: The coastal boundary layer and air pollution- A high temporal resolution analysis in the East Mediterranean Coast, TOASJ, 6 ,9-18,2012.

Uzan, L., Egert, S. and Alpert, P.: Ceilometer evaluation of the eastern Mediterranean summer boundary layer height–first study of two Israeli sites. Atmos. Meas. Tech., 9(9), 4387-4398, 2016.

Vaisala ceilometer CL31 user's guide M210482EN-B, October, 2004.

Wiegner M. and Gasteiger J.: Correction of water vapor absorption for aerosol remote sensing with ceilometers, Atmos. Meas. Tech., 8, 3971–3984, 2015.

Wiegner, M., Madonna, F., Binietoglou, I., Forkel, R., Gasteiger, J., Geiß, A., Pappalardo, G., Schäfer, K. and Thomas, W.: What is the benefit of ceilometers for aerosol remote sensing? An answer from EARLINET, Atmos. Meas. Tech., 7(7), 1979–1997, 2014.

Winker, D.M., Vaughan, M.A., Omar, A., Hu, Y., Powell, K.A., Liu, Z., Hunt, W.H. and Young, S.A.: Overview of the CALIPSO mission and CALIOP data processing algorithms. Journal of Atmospheric and Oceanic Technology, 26(11), 2310-2323, 2009.

Table 1. A list of publications on the September 2015 dust event

Publications	Title	Main Tool	Main outcome
Pu, B. and Ginoux, P (2016)	The impact of the Pacific Decadal Oscillation on springtime dust activity in Syria	MODIS Terra MODIS Aqua DOD AOD, GFDL-AM3 model	Model underestimation in the EM due to inaccurate soil moisture
Parolari et al. (2016)	Climate, not conflict, explains extreme Middle East dust storm.	WRF model	Unusual low level westerly wind spread to the EM, to reversely transport the previously eastward particles back to the EM.
Mamouri et al. (2016)	Extreme dust storm over the eastern Mediterranean in September 2015: satellite, LIDAR, and surface observations in the Cyprus region.	MODIS, EARLINET profiles and PM10	Dust plumes from Syria entered the EM in a double layer structure, pointing to multiple dust sources
Solomos et al. (2016)	Remote sensing and modeling analysis of the extreme dust storm hitting Middle East and Eastern Mediterranean in September 2015.	RAMS model EARLINET LIDAR, MSG and CALIPSO.	Low model ability to simulate the event, due to inaccuracies in model physical processes.
Gasch et al. (2017)	An analysis of the September 2015 severe dust event in the Eastern Mediterranean.	ICON-ART model	An unusual early active Red Sea Trough with meso-scale convective systems generating cold-pool outflows producing the dust storm. Model lacked development of a super critical flow to produce excessive wind speeds.
Jasim, F.H. (2016)	Investigation of the 6-9 September 2015 Dust Storm over Middle East.	Satellite MSG-SEVIRI, Meteoinfo model	Two dust storms simultaneously, from northern Syria and Sinai desert created by two low pressure systems.

Table 2. Ceilometer CL31 locations

Location	Site	Long/Lat	Distance from shoreline (km)	Height (m AGL)
Mount Meron	Northern	33.0/35.4	31	1,150
Ramat David	Northern	32.7/35.2	24	50
Hadera	Onshore	32.5/34.9	3.5	10
Tel Aviv	Onshore	32.1/34.8	0.05	5
Beit Dagan	Inland	32.0/34.8	7.5	33
Weizmann	Inland	31.9/34.8	11.5	60
Nevatim	Southern	31.2/34.9	44	400
Hazerim	Southern	31.2/34.7	70	200

Table 3. Some detail on Israel and Cyprus radiosonde detail

Site	# Station	Lon/Lat	Height (m ASL)	Launching time (UTC)
Israel	40179	34.8/32.0	35	00:00 , 12:00
Cyprus	17607	33.4/35.2	161	06:00 , 12:00

Table 4. Numbers & heights of PM10 measurement sites

Region	Total Number of Stations	Highest Station (m ASL)	Lowest Station (m ASL)
East	9	960	57
Center	16	305	21
Shoreline	12	75	0
South	1	133	133